Vanishing resonances and excited populations: The 4*d* photoabsorption spectrum of Xe-like La^{3+} and I-like La^{4+}

N. Murphy, A. Cummings, P. Dunne, and G. O'Sullivan
School of Physics, University College Dublin, Belfield, Dublin 4, Ireland
(Received 6 November 2006; published 19 March 2007)

The photoabsorption spectrum of Xe-like La^{3+} and I-like La^{4+} has been obtained in the extreme ultraviolet (euv) spectral region with the dual laser produced plasma technique. Photoexcitation from the 4*d* subshell is the dominant process in the 80–150 eV energy range. Strong discrete structure, corresponding to $4d \rightarrow np$, mf ($n>6$, $m>4$) transitions in La^{3+} was observed at lower laser power densities, but with increasing laser flux the discrete features were suppressed and replaced by broad features in the $4d \rightarrow 5p$ and $4d \rightarrow 4f$ regions. This behavior can be attributed to the presence of absorption from excited states containing open 5*p* and 4*f* subshells in La^{3+} and the onset of similar absorption in La^{4+}.

DOI: 10.1103/PhysRevA.75.032509 PACS number(s): 32.30.Jc, 32.80.Dz, 32.80.Fb

I. INTRODUCTION

Since the initial experiment of Lucatorto *et al.* [1] on the photoabsorption of Ba^{+} and Ba^{2+} there has been ongoing interest, both theoretical and experimental, in changes in 4*d* photoabsorption spectra with increasing ionization along the Xe isoelectronic sequence. Above the 4*d* threshold, the Xe photoabsorption spectrum is dominated by a broad $4d \rightarrow \epsilon f$ resonance while below threshold discrete transitions which arise from $4d \rightarrow np$ excitation have been identified ([2–5] and references therein). Transitions of the type $4d \rightarrow nf$ are absent because of the large centrifugal repulsion present in the $l=3$ channel which excludes the nf wave functions from the core region [5–7]. In neutral Xe the potential has a double well character and the nf wave functions are eigenstates of the outer well. With increasing ionization the centrifugal barrier is expected to disappear enabling f wave functions to penetrate into the core region. For Xe, the $4d \rightarrow \epsilon f$ resonance persists in spectra in stages up to Xe^{3+}, where a strong line due to $4d \rightarrow 4f$ transition dominates a spectrum consisting of relatively few discrete lines that form a Rydberg-like structure converging on the resonance. In Xe^{4+}, the spectrum is dominated by two discrete $4d \rightarrow 4f$ and $4d \rightarrow 5f$ features, while the same is true of Xe^{5+} and Xe^{6+} though the intensity of the $4d \rightarrow 5f$ transition decreases and the integrated intensity of the $4d \rightarrow 4f$ transitions grows with increasing ionization [8,9]. Many theoretical studies have been made of the transfer of oscillator strength from the continuum to the discrete spectrum with increasing ionization as a result of 4*f* wave-function contraction into the inner well region [10–15]. Experimentally in Cs^{+} and Ba^{2+} $4d \rightarrow nf$ transitions appear and their relative intensity increases with the degree of ionization. A similar increase in the intensity of $4d \rightarrow nf$ transitions along isonuclear sequences has also been observed in a number of experiments, e.g., iodine [16–18], xenon [9,19–21], caesium [22,23], and barium [24,25]. In the Xe sequence, the labeling of the discrete states is very sensitive to the choice of basis since the lowest $4d^9nf$ states are strongly LS coupled and their wave functions are highly term dependent [22,26–28]. In a multiconfiguration Hartree-Fock (MCHF) average energy of configuration (E_{av}) calculation, the $4d^9nf$ terms are very highly mixed and each $4d^9nf$ level has a small $4d^9 4f_{av}\ ^1P$ component. The $4f_{av}$ function is localized in the core region, i.e., has collapsed, and has a large spatial overlap with the 4*d* wave function. As a result, the different $4d^{10} \rightarrow 4d^9nf$ transitions have appreciable oscillator strength and are generally stronger than the $4d \rightarrow np$ lines. With increasing ionization, the inner potential well becomes deeper and narrower, the barrier disappears, and the 4*f* better approximates a $4f_{av}$ function. Although the higher nf levels have an antinode in this region [29] the level separation increases rapidly so that the nf ($n>4$), $4f_{av}$ mixing diminishes and the oscillator strength becomes concentrated in the $4d^{10} \rightarrow 4d^9 4f\ ^1P_1$ transition. Thus the degree of 4*f* collapse should determine the intensity distribution amongst the observed $4d \rightarrow nf$ transitions until eventually one very strong line should dominate the subthreshold spectrum [14,30].

In an experiment to observe this feature in La^{3+}, Hansen *et al.* [31] found that the $4d^{10} \rightarrow 4d^9 4f\ ^1P_1$ transition was surprisingly absent even though the $4d^{10} \rightarrow 4d^9nf\ ^1P_1$ ($n>4$) transitions appeared as strong relatively sharp lines. They conjectured that since the nonradiative decay rate is determined by the electrostatic $R^k(4f5p, 4d\epsilon l)$ integral and so by the degree of 4*d*, 4*f* overlap, the absence of this transition was due to the width of the feature and the consequent lack of contrast on the photographic plates used in the experiment. In Cs^{+} and Ba^{2+} the $4d \rightarrow 4f$ lines are relatively narrow indicating that the 4*f* wave function is only partially collapsed. The spectrum of La^{3+} was subsequently found by Köble *et al.* [32] to consist of a broad, intense feature with two pronounced peaks arising from strongly interacting $4d^9 4f\ ^1P_1$ and $4d^9 6p\ ^1P_1$ terms with a width of ~2 eV and a series of weaker $4d \rightarrow nf$ ($n>4$) transitions. Based on previous observations for isonuclear sequences of ions around xenon, one would expect that in progressing from La^{3+} to La^{4+}, the $4d \rightarrow 4f$ feature would become even more intense and that the spectrum of ions along the La isonuclear sequence would be dominated by a single intense line some 2 to 3 eV wide. In the present paper we revisit the La^{3+} spectrum and investigate the situation in La^{4+}. We find contrary to observing strong discrete $4d \rightarrow 4f$ lines the spectra in fact can take on the appearance of those observed in low ion stages and that a structure not unlike that of a $4d \rightarrow \epsilon f$ resonance reappears.

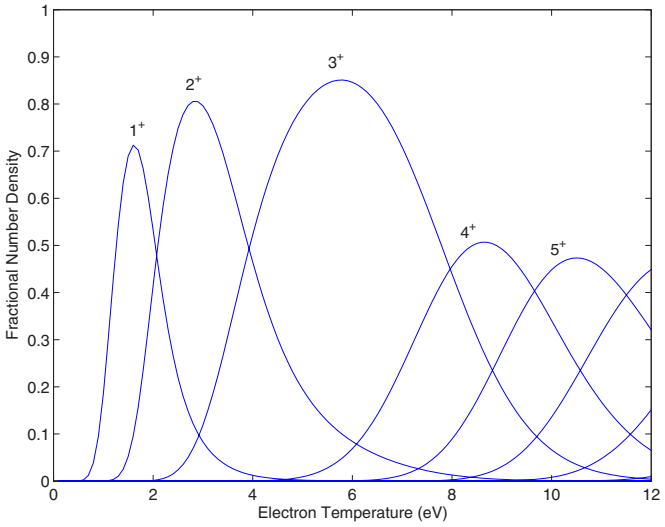

FIG. 1. (Color online) Ion stage distributions for different values of electron temperature in a lanthanum plasma at an electron density of 2×10^{20} cm^{-3}.

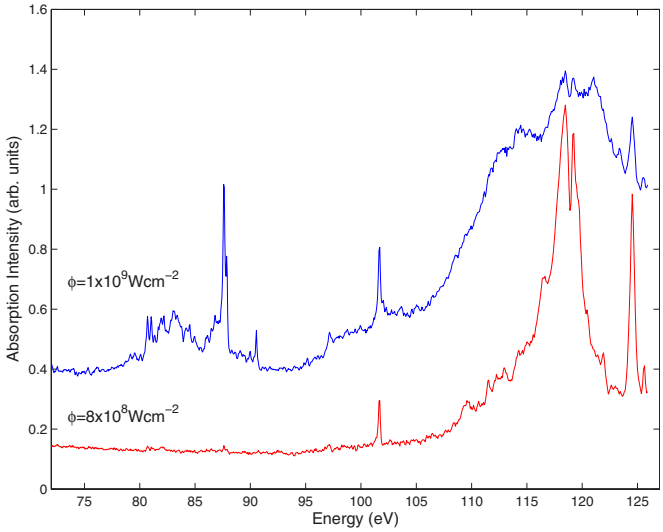

FIG. 2. (Color online) Photoabsorption spectra of a lanthanum plasma recorded using the DLP technique. At a time delay, $\Delta\tau \approx 50$ ns, between the creation of the absorbing pulse and the backlighting plasma the spectrum consists almost exclusively of La IV (bottom spectrum) while at the shorter delay it is due to a mixture of La IV and La V (top spectrum).

II. EXPERIMENT

In our experiments, spectra were recorded photoelectrically on a 0.25 m Jenoptic E-Spec flat field Spectrograph using the dual laser produced plasma (DLP) method. The spectra were recorded on a back thinned calibrated 1024 $\times$1024 pixel charge-coupled device (CCD) detector whose position is fixed and gives a simultaneous energy coverage from 72 to 127 eV. A more detailed account of the DLP method can be found elsewhere [33,34]. In the present experiments, a 700 mJ 10 ns, 1.06 μm Nd:YAG laser pulse was used to provide the backlighting continuum by tightly focusing onto a tungsten target while the absorbing plasma was produced by a 15 ns full width at half maximum (FWHM), Q-switched, 1.06 μm Nd:YAG laser pulse, focused through a cylindrical lens to produce a damage area 9 mm in length and 0.54 mm in width on a planar target of metallic lanthanum. The plasma conditions were altered by either varying the laser pulse energy while maintaining tight focus or keeping the laser energy fixed and changing the focusing conditions, since the plasma electron temperature and hence the degree of ionization is a sensitive function of the laser pulse power density. Using the full laser pulse energy of 900 mJ yielded an average power density, ϕ, of 1.2×10^9 W cm^{-2}. The corresponding electron temperature, calculated from the semiempirical formula of Colombant and Tonon [35] is $\sim$4 eV. However, a more accurate estimate of plasma conditions may be obtained from studying the ion stage distribution. The variation of ion stage with electron temperature, calculated by assuming collisional radiative (CR) equilibrium is presented in Fig. 1. From this figure it is apparent that electron temperatures in the range 3–9 eV are required to produce La^{3+} while the optimum temperature is close to 6 eV. At the shortest time delays it proved possible to obtain stages up to and including La^{6+} which could be readily identified from their $4d\rightarrow5p$ spectra and an analysis of $4d\rightarrow5p$ transitions in La^{4+} through La^{6+} was recently published [36]. The production of closed shell species such as rare gaslike ions is particularly favored in laser plasmas so one would expect relatively large populations of La^{3+}, reflected in Fig. 1 by the relatively large temperature range over which this stage dominates. By recording spectra at a series of different time delays and noting that lower stages appear after increasingly long times, it is possible to infer the contribution from each stage. Further ion stage differentiation can be facilitated by comparison of spectra recorded from different plasma regions by essentially translating the plasma across that portion of the probing extreme ultraviolet (euv) continuum beam which is coincident with the optical axis of the spectrograph.

Data files were provided with the spectrometer giving λ, $\Delta\lambda$, and counts per photon for each row of the CCD array giving a resolving power $\frac{E}{\Delta E}$ between 1300 and 1900 (with decreasing energy). In the spectral region considered here, the average resolving power is 1400 which translates to an energy uncertainty of 0.08 eV. The overall energy uncertainty corresponds to three pixels of the CCD array. Two experimental results, taken with an interlaser delay of 50 ns under the conditions where La^{3+} absorption should dominate the spectrum are shown in Fig. 2. For plasmas formed at slightly lower laser power densities, (7 to 8)$\times10^8$ W cm^{-2}, the spectrum obtained is essentially the same as that observed by Köble *et al.* [32] and is dominated by a strong resonance feature containing overlapping $4d^{10}\rightarrow(4d^9 4f + 4d^9 6p)\ ^1P_1$ transitions, with no strong lines appearing in the $4d\rightarrow5p$ region (at lower energies). Some evidence of absorption by La^+ is also evident in this spectrum and is responsible for the weak structure between 110 and 115 eV and La^{2+} at 116 and 122 eV. For plasmas produced at higher power densities (top spectrum in Fig. 2) a number of lines appear in the $4d\rightarrow5p$ region. The strong lines between 87 and 91 eV were previously identified as arising from absorp-

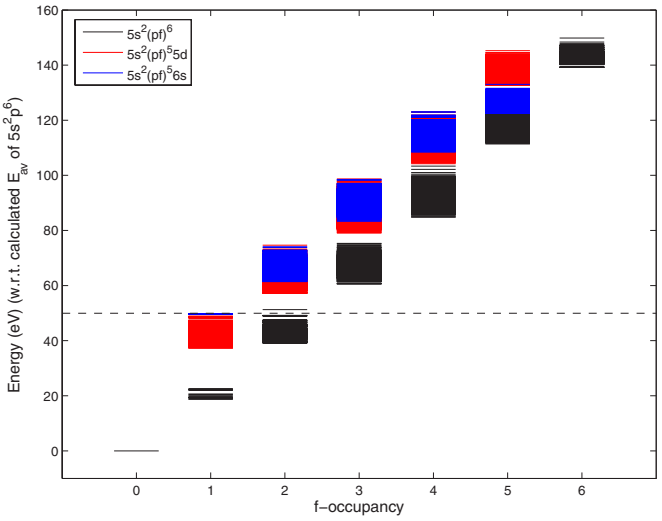

FIG. 3. (Color online) Energy level diagram of the three lowest lying configurations with varying f-occupancy of Xe-like La IV. The average configuration energies were found using HFCI calculations. The dashed line shows the ionization potential (49.95 eV) of La IV.

tion in La^{4+} [36] and the structure between 82 and 85 eV is also calculated to arise from the same ion stage. The additional structure appearing at 82–81.5 eV and 86–88 eV can be attributed to La^{3+}. Moreover, in these spectra the La^{3+} $4d \rightarrow 5f$ line identified earlier [32] is also strongly in evidence. However, the $4d \rightarrow 4f$ feature appears within a broad resonancelike peak some 10 eV wide.

III. RESULTS

Up to now one critical aspect of $4f$ electron behavior has been ignored. For ions isoelectronic with Xe, center of gravity calculations performed with the Froese Fischer HF code [37] predicted that the ground configuration changes with increasing ionization from $5s^25p^6$ to $5s^25p^44f^2$ at Pm VIII, to $5s^24f^6$ at Eu X, and eventually to $4f^8$ at Ho XIV as a result of $4f$ wave-function contraction. Indeed subsequent calculations with the Cowan code [38] predicted that arising from the near degeneracy of the resulting configurations, at $Z=62$ configuration interaction completely mixes the resulting states and nl labels become meaningless. In lower ion stages this process leads to the appearance, at relatively modest energies, of configurations containing variable numbers of $4f$ and $5p$ electrons. The effects on the spectral profile of autoionizing $4d \rightarrow 4f$ transitions in the presence of bound $4f$ electrons has been discussed by Combet-Farnoux [39]. Many of the resulting terms possess large J values and so can contain a non-negligible fraction of the total ion population at the plasma temperatures necessary to generate the required ion stage. The locations of the calculated [average configuration energies from Hartree Fock with configuration interaction (HFCI) code [40]] lowest lying terms of these configurations are shown in Fig. 3. From this figure it is obvious that the increase in $4f$ binding energy relative to the $5p$ means that configurations such as $5p^54f$ and $5p^44f^2$ gradually approach the $4f^6$ as one proceeds along the sequence in La^{3+}. The $5p^54f$ configuration lies some 17.8 eV above the $5p^6\ {}^1S_0$ and the $5p^44f^2$ about 40 eV higher. The lowest level of the $5p^55d$ is 19.4 eV above the ground state, and the $5p^54f$ and $5p^55d$ configurations overlap in energy and extend upwards to 27 eV above it [41,42]. Since the plasma electron temperatures in the range 3–9 eV are required to produce a significant population of La^{3+}, the lowest $5p^54f$ and $5p^55d$ configurations will have significant populations especially in light of their multiplicities. In our other work, it was shown that a Boltzmann distribution gives a good estimate of the population distribution within a given ion stage. Moreover, the gA values (transition rates) of $5d \rightarrow 4f$ transitions are of the order of microseconds compared to the plasma duration of tens of nanoseconds so that populations are essentially established by collision and capture processes. Since ions with singly excited configurations with higher nl $(n>5)$ electrons have larger radii, the collisional ionization and excitation rate for these is significantly enhanced relative to configurations based on $n=4$ and 5 electrons only. Therefore in estimating excited state populations it was considered reasonable to confine the calculations to the configurations $5p^k$, $5p^{k-1}4f$, $5p^{k-1}5d$, and $5p^{k-2}4f^2$ ($k=6$ and 5 for La IV and La V, respectively). Because of the high J values possible for the latter and its position (40 eV above the ground state) the contribution from this configuration becomes significant at higher electron temperatures. In order to predict the energies of these configurations and the associated discrete features expected for $4d \rightarrow np, mf$ transitions, Hartree Fock with configuration interaction (HFCI) calculations were performed with the RCN, RCN2, and RCG suite of programs developed by Cowan [40]. In this method, wave functions are first determined in an LS coupled configuration interaction calculation using an excited state basis which consisted of $4d^9$ $[5s^25p^k + 5s^25p^{k-1}5d + 5s^25p^{k-1}4f + 5s^25p^{k-2}4f^2]$ np, mf with $5 \leqslant n \leqslant 7$, $4 \leqslant m \leqslant 7$ and a discretized continuum where $k=6$ for La IV and $k=5$ for La V. Then the energy level positions, oscillator strengths, and linewidths were subsequently determined in an intermediate coupling scheme. These calculations gave excellent agreement with both the experimental data and calculations of Köble *et al.* [32] for scaling factors of 75% for the Slater Condon F^k, G^k, and R^k *ab initio* parameters. In line with the earlier calculations the spin orbit parameters ζ_k were not adjusted except for the $4d^{10}5s^25p^5 \rightarrow 4d^95s^25p^6$ transition of La V where the spin orbit integral ζ_{4d} was scaled to 102%. This gave optimum agreement between theory and experiment for $4d \rightarrow 5p$ transitions [36]. Since the excited states decay primarily by nonradiative processes the cross section has been calculated assuming a Lorentzian line profile using the formula $\sigma(\mathrm{Mb}) = 109.7\Gamma_k f_k \left[2\pi\left((E_k-E)^2+\frac{\Gamma_k^2}{4}\right)\right]^{-1}$ where E_k and Γ_k are the calculated energy and calculated linewidth of the transition (in eV) and f_k is the absorption oscillator strength. In order to calculate σ it is also necessary to evaluate the decay linewidth, Γ, resulting from allowed autoionization processes. The dominant nonradiative decay mechanisms for inner shell $4d$ holes following $d \rightarrow p$ or $d \rightarrow f$ excitation for the lowest energy configurations are

$$4d^95s^25p^knl \rightarrow 4d^{10}5s^25p^{k-1} + \epsilon l'$$

TABLE I. Populations of low lying configurations in La IV ($k=6$) and La V ($k=5$) at $T_e=3$ and 8 eV.

	La^{3+}		La^{4+}	
Configuration	$T_e=3$ eV (%)	$T_e=8$ eV (%)	$T_e=3$ eV (%)	$T_e=8$ eV (%)
$5s^25p^k$	99.0	85.7	99.6	94.8
$5s^25p^{k-1}4f$	0.7	7.2	0.4	2.9
$5s^25p^{k-1}5d$	0.3	6.6	0.0	2.0
$5s^25p^{k-2}4f^2$	0.0	0.5	0.0	0.3

$$(l' = 0,2,4,6 \text{ if } l = 3 \text{ and } 0,2,4 \text{ if } l = 1),$$

$$4d^95s^25p^knl \rightarrow 4d^{10}5s^15p^k + \epsilon l'$$

$$(l' = 1,3,5 \text{ if } l = 3 \text{ and } 1 \text{ if } l = 1),$$

$$4d^95s^25p^knl \rightarrow 4d^{10}5s^25p^{k-2}nl + \epsilon l'(l' = 0,2,4)$$

$$\rightarrow 4d^{10}5s^15p^{k-1}nl + \epsilon l'(l' = 1,3)$$

$$\rightarrow 4d^{10}5s^05p^knl + \epsilon l'(l' = 2).$$

With increasing ion stages these different processes cease to be energetically feasible and the last process here is disallowed for in all the ion stages presented in this paper. For $4d$ excitation from excited state configurations involving $5d$ or multiple $4f$ electrons additional decay channels became available and where possible these were accounted for in the calculations. Cross sections were then evaluated for the different terms of the $5p^6$, $5p^54f$, $5p^55d$, and $5p^44f^2$ configurations of La IV. A normalized Boltzmann distribution was assumed with the ground configuration and the relative contribution from each term from the above configurations was evaluated and absorption profiles for a range of electron temperatures were produced. The relative importance of the different parent configurations may be assessed from Table I. These profiles were then convolved with a Gaussian (FWHM) instrumental function using the calibration data given with the euv spectrometer. These are shown in Fig. 4. In producing this figure, the steady state collisional radiative (CR) model of Colombant and Tonon [35] was used to predict the percentage component of each ion present for each electron temperature for an electron density of 2×10^{20} cm^{-3}. The calculated decay widths from the allowable autoionization processes were used in the energy range 75–95 eV for each individual configuration. However, due to the added complication of transitions coming from open f shells (in both ion stages), the decay widths were averaged over the strongest 40 lines in the energy range 95–126 eV region. The broadest averaged decay width encountered in this work was 2.02 eV associated with decays from the $4d^95s^25p^34f^3$ configuration of La V. For La V, the ground configuration is $5s^25p^5$ and the lowest excited states are $5s^25p^44f$, $5s^25p^45d$, and $5s^25p^34f^2$. The lowest term of the $5s^25p^45d$ lies at 20.7 eV and the configuration extends upwards to 29.4 eV [43] while the $5s^25p^44f$ configuration is predicted to extend from 16.0 to 23.7 eV and the $5s^25p^34f^2$ ranges from 36.3 to 48.7 eV. As in the case for La IV, excited state absorption followed by autoionization was allowed for as well as absorption from the spin-orbit split ground configuration, the cross sections were weighted with Boltzmann and CR factors for a range of electron temperatures and then convolved with a Gaussian instrumental function (Fig. 4). Two things are immediately obvious from these data. First, the overall effect is that the oscillator strength envelope of the strongest transitions is seen to remain close to the $4d^{10} \rightarrow 4d^94f\ ^1P_1$ peak though it shows considerable evidence of structure and the FWHM increases with temperature as the contribution of excited configurations increases. Second, substantial structure appears due to $4d^{10}5p^k(4f+5d) \rightarrow 4d^95p^{k+1}(4f+5d)$ transitions in the lower energy region where $k=5$ for La IV and $k=4$ for La V. Thus under the conditions necessary to obtain La^{3+} absorption in a DLP experiment it is somewhat surprising to obtain a purely ground state population of ions. Two synthetic spectra were generated, one at an electron temperature of 3 eV and the other for an 8 eV electron temperature. These temperatures gave optimum agreement with the experimental spectra shown in Fig. 2. The resulting synthetic spectra are shown in Figs. 5 and 6 where they are compared to experimental data. In both cases the theoretical spectra were weighted according to the relative populations for La^{3+} and La^{4+} ions as obtained in the CR model. As explained earlier, Fig. 5 consists predominantly of La^{3+} while Fig. 6 consists of equal populations of La^{3+} and La^{4+} which is expected for an electron temperature of 8 eV (see Fig. 1).

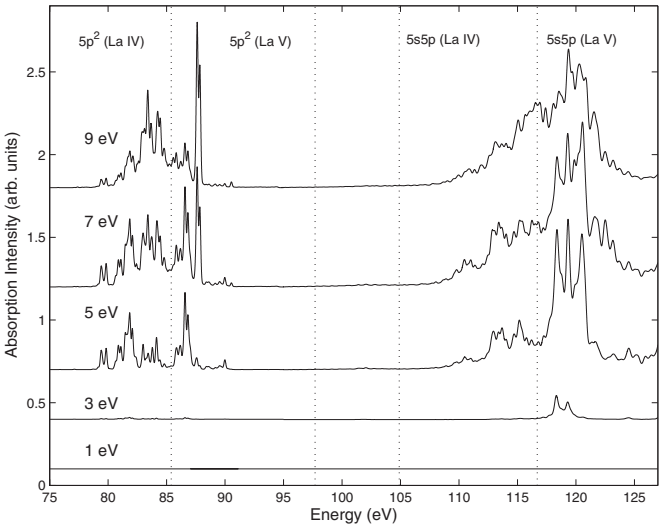

FIG. 4. Variation in the calculated absorption profile as a function of electron temperature assuming a normalized Boltzmann distribution amongst the terms of the configurations of La IV and La V. These spectra were convolved with a Gaussian (FWHM) instrumental function and also weighted by the factors given by the steady state collisional radiative (CR) model of Colombant and Tonon [35] for each ion stage and temperature. The dashed vertical lines show the approximate thresholds for $5p^2$ and $5s5p$ double electron excitations for both ions.

In Fig. 6 comparison is made with the results of calculations for transitions from the ground and excited state con-

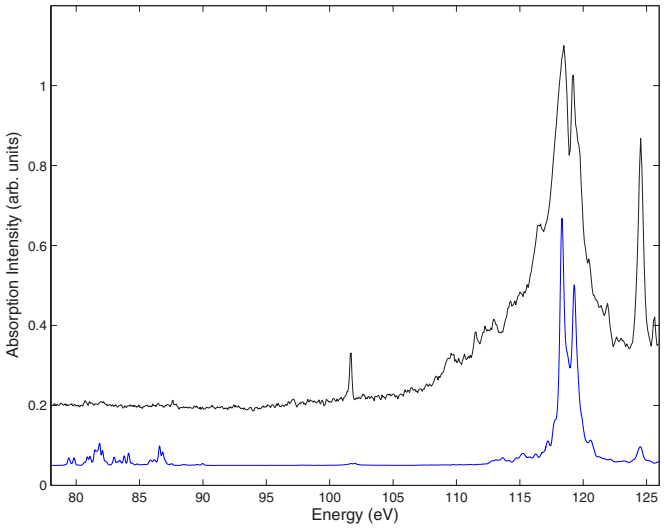

FIG. 5. (Color online) The photoabsorption spectrum (top) of predominantly La^{3+} compared with the results of HFCI calculations (bottom) for an electron temperature of 3 eV. Cross sections were calculated for each of the component terms of the ground and excited configurations of La IV and La V, then weighted and summed assuming a normalized Boltzmann distribution amongst the excited states and ion ratios obtained from the CR model and the convolved with then Gaussian instrumental function to obtain an absorption profile. The plasma composition is 81% La^{3+} and 1% La^{4+}. Note: The $4f\,^3D$ feature (calculated decay width of 0.04 eV) at 101.6 eV is not present in the synthetic spectrum as the calculated decay width of 0.7 eV for the strongest $4d^{10}\rightarrow 4d^9 4f\,^1P_1$ transition was assigned to all $4d^{10}\rightarrow 4d^9 4f$ transitions in generating this spectrum.

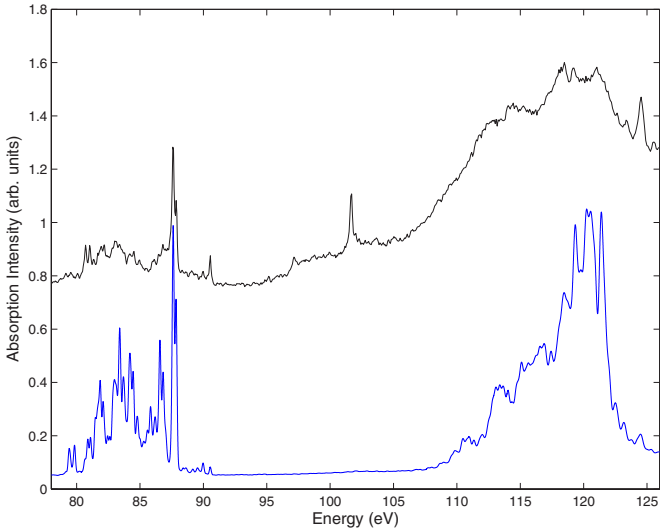

FIG. 6. (Color online) The photoabsorption spectrum (top) of predominantly La^{3+} and La^{4+} compared with the results of HFCI calculations (bottom) for an electron temperature of 8 eV. Cross sections were calculated for each of the component terms of the ground and excited configurations of La IV and La V, then weighted and summed assuming a normalized Boltzmann distribution amongst the excited states and ion ratios obtained from the CR model and convolved with the Gaussian instrumental function to obtain an absorption profile. The fractional contribution of La^{3+} and La^{4+} is 45% for each. Note: The $4f\,^3D$ feature (calculated decay width of 0.04 eV) at 101.6 eV is not present in the synthetic spectrum as the calculated decay width of 0.7 eV for the strongest $4d^{10}\rightarrow 4d^9 4f\,^1P_1$ transition was assigned to all $4d^{10}\rightarrow 4d^9 4f$ transitions in generating this spectrum.

figurations of La^{3+} and La^{4+} and the experimentally obtained spectrum. It is seen that good agreement is obtained for an electron temperature of 8 eV. The strong features at 87.6, 87.7, and 90.5 eV have been previously identified by Murphy *et al.* [36] as $4d^{10}5s^25p^5\rightarrow 4d^95s^25p^6$ transitions of La V. The rest of the structure between 78 and 90 eV is predominantly due to $4d^{10}5s^25p^k[4f+5d]\rightarrow 4d^95s^25p^{k+1}[4f+5d]$ transitions where $k=5$ for La^{3+} and $k=4$ for La^{4+}. In the $4d\rightarrow 4f$ region (100–126 eV), again the $4d^{10}5p^k4f\rightarrow 4d^95p^k4f^2$ transitions contribute on the low energy side of the $4d^{10}\rightarrow 4d^94f\,^1P_1$ feature while the $4d^{10}5p^k5d\rightarrow 4d^95p^k4f5d$ contributes on the high energy side ($k=5$ for La^{3+} and $k=4$ for La^{4+}). The effect of the $4d^{10}5p^k4f^2\rightarrow 4d^95p^k4f^3$ lines is largely to smooth out the resonance where $k=4$ for La^{3+} and $k=3$ for La^{4+}.

IV. CONCLUSION

We have shown that the population of excited metastable states, arising as a direct consequence of $4f$ orbital contraction completely alters the $4d$ photoabsorption spectra along the La isonuclear sequence compared to that of Xe. Instead of a single line, a broad shape resonancelike feature reappears. Such behavior should also frustrate the smooth transition from the $4d\rightarrow\epsilon f$ resonance to $4d\rightarrow 4f$ transitions predicted for the Xe isoelectronic sequence. It is known that the sequence effectively terminates in emission at Nd^{6+} [44], it is reasonable to assume that certainly for the DLP method, the temperatures required to produce even the next ion, Ce^{4+}, will be sufficient to populate a sizeable fraction of excited states as they converge on the $5p^6$ ground configuration. The behavior is thus determined by two factors; the reduction in energy spread of the excited configurations with increasing ionization and the need for higher energies to produce these ions. We are currently investigating this behavior in Ce^{4+}. It is also interesting to note that in the experimental spectrum of La IV produced by Hansen *et al.* [31], their laser power density of 9×10^8 W cm^{-3} is between the two extremes shown here in Figs. 5 and 6. It is likely that metastable states from both La^{3+} and La^{4+} contributed to their experimental spectrum smoothing out the already broad $4d^{10}\rightarrow 4d^9 4f\,^1P_1$ feature leading to another possible explanation as to why the resonance was not observed.

ACKNOWLEDGMENT

This work was supported by Science Foundation Ireland under Investigator Grant No. 02/IN.1/I99.

[1] T. B. Lucatorto, T. J. McIlrath, J. Sugar, and S. M. Younger, Phys. Rev. Lett. **47**, 1124 (1981).
[2] R. Haensel, G. Keitel, P. Schreiber, and C. Kunz, Phys. Rev. **188**, 1375 (1969).
[3] U. Becker, D. Szostak, H. G. Kerkhoff, M. Kupsch, B. Langer, R. Wehlitz, A. Yagishita, and T. Hayaishi, Phys. Rev. A **39**, 3902 (1989).
[4] V. Schmidt, Rep. Prog. Phys. **55**, 1483 (1992).
[5] J. P. Connerade, *Highly Excited Atoms* (Cambridge University Press, Cambridge, England, 1999).
[6] J. W. Cooper, Phys. Rev. Lett. **13**, 762 (1964).
[7] J. P. Connerade, Contemp. Phys. **19**, 415 (1978).
[8] J. M. Bizau, C. Blancard, D. Cubaynes, F. Folkmann, J. P. Champeaux, J. L. Lemaire, and F. J. Wuilleumier, Phys. Rev. A **73**, 022718 (2006).
[9] A. Aguilar, J. D. Gillaspy, G. F. Gribakin, R. A. Phaneuf, M. F. Gharaibeh, M. G. Kozlov, J. D. Bozek, and A. L. D. Kilcoyne, Phys. Rev. A **73**, 032717 (2006).
[10] R. I. Karaziya, Sov. Phys. Usp. **24**, 775 (1981).
[11] K. Nuroh, M. J. Stott, and E. Zaremba, Phys. Rev. Lett. **49**, 862 (1982).
[12] G. O'Sullivan, J. Phys. B **15**, L765 (1982).
[13] S. Kučas, A. Kariosiene, and R. Karaziya, Sov. Phys. Collect. **28**, 36 (1983).
[14] K. T. Cheng and C. Froese Fischer, Phys. Rev. A **28**, 2811 (1983).
[15] A. T. Domondon and X. M. Tong, Phys. Rev. A **65**, 032718 (2002).
[16] G. O'Sullivan, C. McGuinness, J. T. Costello, E. T. Kennedy, and B. Weinmann, Phys. Rev. A **53**, 3211 (1996).
[17] H. Kjeldsen, P. Andersen, F. Folkmann, H. Knudsen, B. Kristensen, J. B. West, and T. Andersen, Phys. Rev. A **62**, 020702(R) (2000).
[18] H. Kjeldsen, P. Andersen, F. Folkmann, J. E. Hansen, M. Kitajima, and T. Andersen, J. Phys. B **35**, 2845 (2002).
[19] M. Sano, Y. Itoh, T. Koizumi, T. M. Kojima, S. D. Kravis, M. Oura, T. Sekioka, N. Watanabe, Y. Awaya, and F. Koike, J. Phys. B **29**, 5305 (1996).
[20] N. Watanabe *et al.*, J. Phys. B **31**, 4137 (1998).
[21] P. Andersen, T. Andersen, F. Folkmann, V. K. Ivanov, H. Kjeldsen, and J. B. West, J. Phys. B **34**, 2009 (2001).
[22] A. Cummings and G. O'Sullivan, J. Phys. B **30**, 5599 (1997).
[23] A. Cummings, C. McGuinness, G. O'Sullivan, J. T. Costello, J. P. Mosnier, and E. T. Kennedy, Phys. Rev. A **63**, 022702 (2001).
[24] T. Koizumi, Y. Itoh, M. Sano, M. Kimura, S. Kravis, A. Matsumoto, M. Oura, T. Sekioka, and Y. Awaya, J. Phys. B **28**, 609 (1995).
[25] J. M. Bizau *et al.*, Phys. Rev. Lett. **87**, 273002 (2001).
[26] J. P. Connerade and M. W. D. Mansfield, Phys. Rev. Lett. **48**, 131 (1982).
[27] C. W. Clark, J. Phys. B **1**, 626 (1984).
[28] S. Kučas and R. Karaziya, Phys. Scr. **58**, 220 (1998).
[29] G. Wendin and A. F. Starace, J. Phys. B **11**, 4119 (1978).
[30] K. T. Cheng and W. R. Johnson, Phys. Rev. A **28**, 2820 (1983).
[31] J. E. Hansen, J. Brilly, E. T. Kennedy, and G. O'Sullivan, Phys. Rev. Lett. **63**, 1934 (1989).
[32] U. Köble, L. Kiernan, J. T. Costello, J. P. Mosnier, E. T. Kennedy, V. K. Ivanov, V. A. Kupchenko, and M. S. Shendrik, Phys. Rev. Lett. **74**, 2188 (1995).
[33] J. T. Costello, E. T. Kennedy, J. P. Mosnier, P. K. Carroll, and G. O'Sullivan, Phys. Scr., T **34**, 77 (1991).
[34] E. T. Kennedy, J. T. Costello, J. P. Mosnier, and P. van Kampen, Radiat. Phys. Chem. **70**, 291 (2004).
[35] D. Colombant and G. F. Tonon, J. Appl. Phys. **44**, 3524 (1973).
[36] N. Murphy, A. Cummings, G. O'Sullivan, and P. Dunne, J. Phys. B **39**, 3087 (2006).
[37] C. F. Fischer, Comput. Phys. Commun. **1**, 151 (1969).
[38] G. O'Sullivan, P. K. Carroll, P. Dunne, R. Faulkner, C. McGuinness, and N. Murphy, J. Phys. B **32**, 1893 (1999).
[39] F. Combet-Farnoux, *Proceedings of a NATO Advanced Study Institute on Giant Resonances in Atoms, Molecules and Solids* edited by J. P. Connerade, J. M. Esteva, and R. C. Karnatak (Plenum Press, New York, 1987), Vol. 151.
[40] R. D. Cowan, *The Theory of Atomic Structure and Spectra* (University of California Press, Berkley, 1981).
[41] J. Reader and G. L. Epstein, J. Opt. Soc. Am. **65**, 638 (1975).
[42] W. C. Martin, R. Zalubas, and L. Hagan, *Atomic Energy Levels-The Rare-Earth Elements* (National Bureau of Standards, Washington, D.C., 1980).
[43] G. L. Epstein and J. Reader, J. Opt. Soc. Am. **66**, 590 (1976).
[44] B. Edlén, Phys. Scr. **7**, 93 (1973).